Deep Space Tracking in Local Reference Frames

R. N. Treuhaft
Tracking Systems and Applications Section

A self-calibrating deep space tracking technique is described which can potentially produce 2-nanoradian angular spacecraft determinations. The technique uses very long baseline interferometric observations of a spacecraft and several radio sources. This article first describes the currently employed single-source technique as a parameter estimation procedure. Extending the number of parameters and observations leads to the proposed local reference frame technique. Station clock, Earth rotation, and tropospheric parameters are estimated along with spacecraft position from the multisource observation sequence. The contributions to spacecraft angular uncertainty from system noise, tropospheric fluctuations, and uncalibrated radio source structure are evaluated. Of these experimental errors, radio source structure dominates the determination of the spacecraft position in the radio reference frame. It is shown, however, that the sensitivity of relative spacecraft position accuracies to time-invariant radio source structure effects may be on the order of 2 nanoradians.

I. Introduction

Deep space angular tracking is routinely performed on Voyager with 50- to 100-nanoradian accuracy [1] and will be performed on Galileo at the 50-nanoradian level. The analysis in this article suggests a tracking strategy for the Deep Space Network (DSN) which, in the 30-minute measurement time typically allotted for angular tracking, will potentially yield better than 2-nanoradian accuracy and will require virtually no calibration support external to the signal chains at the stations. The self-calibrating technique outlined below capitalizes on the extreme sensitivity of the DSN after it is equipped with Mark III observing bandwidths and recording hardware [2].

The proposed astrometric technique can potentially determine angular distances accurate to 10 km near Neptune, or 2 km near Jupiter. Such a capability would allow the determination of a planet's position in the radio frame by sensing gravitational forces long before encounter [3].[1] In addition to providing navigational benefits, the technique to be described would help the DSN realize its potential as a high-precision astrometric radio and planetary science tool. This astrometric technique would facilitate other tracking-related scientific measurement, such as the determination of planetary and satellite masses. Additional experiments, such as direct measurement of relativistic gravitational bending by Jupiter would also become possible.

[1] R. N. Treuhaft and J. S. Ulvestad, "Using Gravitational Signatures for Target-Relative Angular Tracking During Planetary Approach," JPL Interoffice Memorandum No. 335.3-88-76 (internal document), Jet Propulsion Laboratory, Pasadena, California, July 11, 1988.

Angular deep space navigation is currently achieved by tracking with Very Long Baseline Interferometry (VLBI) [4]-[6]. In a technique called Delta Differential One-Way Range (ΔDOR), the geometric delay of a radio source signal is differenced from that of a spacecraft signal [1]. Through this difference, the angular stability of the radio reference frame, determined by the accuracy of the radio source catalog, can be transferred to the spacecraft angular measurement. For the DSN astrometric radio catalog, measurement errors currently limit radio source astrometry to the 10-nanoradian level [7]. As measurement techniques and instrumentation improve, source structure variability will begin to limit astrometric accuracy at the 5-nanoradian level [8].

In practice, the current 10-nanoradian stability of the radio frame is not completely transferred to the spacecraft angular accuracy. Errors in the determination of the spacecraft and radio source delays at the time of the ΔDOR measurement limit tracking accuracy to the 20- to 50-nanoradian range, which is about 15 to 40 kilometers of projected error at Jupiter or 90 to 225 kilometers at Neptune [1].[2] It has been shown that 5- to 10-nanoradian accuracies could be achieved with future DSN hardware configurations and improved calibration support using the ΔDOR single radio source technique.[3]

The alternative measurement strategy outlined below entails interferometric observations of a spacecraft and a number of radio sources. This technique of navigation in a local reference frame of radio sources can potentially yield 2-nanoradian accuracy without clock synchronization, Earth orientation, or tropospheric calibration support. The thrust of the local reference frame technique is to use the known positions of several reference radio sources to determine the magnitude of systematic errors affecting the normal ΔDOR position measurement. Navigation in a local reference frame is especially attractive for outer planet missions in which the spacecraft moves by only a few degrees on the sky over a year. For example, Voyager will be in the same 15-square-degree piece of sky from late 1987 until Neptune encounter. An additional advantage of the local reference frame technique is that the radio sources do not have to be angularly close to the spacecraft; 30-degree separations still yield the high accuracy mentioned above. When a spacecraft drifts away from the radio source to which it has been referenced with standard ΔDOR, it will sometimes be in a place where no other close sources are available. The local reference frame technique is ideal in situations in which a "hole" in the known extragalactic radio sky is encountered.

In the next section, the conventional single radio source ΔDOR strategy is reviewed as a parameter estimation process. The local reference frame technique is then developed in Section III as an extension of this process. Section IV contains covariance results for the local network technique as compared to conventional ΔDOR. Section V summarizes the proposed technique, outlines possible improvements, and reports the status of experimental efforts at validation.

II. Delta DOR as Parameter Estimation

In this section, the ΔDOR process will be formulated as parameter estimation from observed VLBI delays. The dependence of the VLBI delays on spacecraft position and clock parameters will be followed by the least squares result for estimating the parameters and their errors. Extending the dependence of observed VLBI delays to include station clock rates, Earth rotation, and tropospheric effects will then lead to the local reference frame technique in the next section.

The object of angular tracking is to determine the spacecraft unit vector, which points from the Earth to the spacecraft. The essential quantities derived from ΔDOR measurements are the components of the residual spacecraft unit vector.[4] With DSN VLBI, these components are determined by observations on nearly orthogonal baselines. The following analysis will treat measurements on a single baseline only. In that case, the quantity to be determined, Δs_p, is the component of the residual spacecraft unit vector along the projected baseline, which is the baseline projected onto the plane of the sky. Given the length of the a priori projected baseline, B_p at the spacecraft observation epoch,

$$\Delta s_p = \frac{c\Delta\tau}{B_p} \tag{1}$$

In Eq. (1), c is the speed of light, and $\Delta\tau_g$ is the residual spacecraft geometric delay. It is given by

$$\Delta\tau_g = \frac{\vec{B}_m \cdot (\hat{s}_{sc} - \hat{s}_{m\,sc})}{c} \tag{2}$$

[2] J. B. Thomas, "An Error Analysis for Galileo Angular Position Measurements With the Block 1 ΔDOR System," JPL Engineering Memorandum No. 335-26 (internal document), Jet Propulsion Laboratory, Pasadena, California, November 11, 1981.

[3] R. N. Treuhaft and L. J. Wood, "Revisions in the Differential VLBI Error Budget and Applications for Navigation in Future Missions," JPL Interoffice Memorandum No. 335.4-601 (internal document), Jet Propulsion Laboratory, Pasadena, California, December 31, 1986.

[4] The term *residual* used in the analysis means the difference between the actual value of a quantity and its best known a priori value. Residuals are used both to linearize subsequent least squares procedures and to make computation less cumbersome.

where $\vec{B}_m$ is the total baseline vector at the epoch of the spacecraft measurement, $\hat{s}_{sc}$ is the actual unit vector pointing to the spacecraft, and $\hat{s}_{m\,sc}$ is the a priori spacecraft unit vector. In much of the following analysis, $\Delta\tau_g$ will be regarded as the quantity to be determined from the interferometric observations. Geometric delays are related to projected spacecraft angles via Eq. (1). The rest of this section is devoted to the procedure for estimating $\Delta\tau_g$ and its error.

The extraction of $\Delta\tau_g$ from ΔDOR observations can be viewed as a simple example of parameter estimation. In Eqs. (3) and (4) below, the observed spacecraft and radio source residual delays, $\Delta\tau_{sc}$ and $\Delta\tau_{rs}$, are expressed in terms of $\Delta\tau_g$ and the residual difference between clock epochs at the two observing stations, $\Delta\tau_c$:

$$\Delta\tau_{sc} = \frac{\partial\tau_{sc}}{\partial\tau_g}\Delta\tau_g + \frac{\partial\tau_{sc}}{\partial\tau_c}\Delta\tau_c + \epsilon_{sc} \tag{3}$$

$$\Delta\tau_{rs} = \frac{\partial\tau_{rs}}{\partial\tau_c}\Delta\tau_c + \epsilon_{rs} \tag{4}$$

where ϵ_{sc} represents all contributions to observed spacecraft delay not included in the first two terms on the right side of Eq. (3). Similarly, ϵ_{rs} represents all effects not included in the first term on the right of Eq. (4). Since both $\Delta\tau_g$ and $\Delta\tau_c$ are delays, they map directly into observed residual delays, and all partial derivatives in Eqs. (3) and (4) are unity. Note that a residual radio source geometric delay, analogous to Eq. (2), does not explicitly appear in Eq. (4). This is because the residual delay effects induced by errors in the a priori baseline components and radio source coordinates are included in ϵ_{sc} and ϵ_{rs}. The only delay terms which explicitly appear in Eqs. (3) and (4) are those which contain parameters to be estimated. Generally, both random and systematic effects are included in ϵ_{sc} and ϵ_{rs}, but in the following discussion they are both assumed to have zero mean statistics.

Standard least squares procedures (e.g., [9]) give the minimum variance estimates of $\Delta\tau_g$ and $\Delta\tau_c$, $\widehat{\Delta\tau}_g$ and $\widehat{\Delta\tau}_c$, in terms of the observed residual delays:

$$\widehat{\Delta\tau}_g = \Delta\tau_{sc} - \Delta\tau_{rs} \tag{5}$$

$$\widehat{\Delta\tau}_c = \Delta\tau_{rs} \tag{6}$$

Equation (5) gives the familiar prescription of differencing the spacecraft and radio source observed residual delays to estimate $\Delta\tau_g$. The estimate of clock epoch given in Eq. (6) is available for correcting time tags in other radio metric data. The parameter estimate variances due to white observable noise are also determined by standard least squares methods. For ΔDOR, with the dependence of observables on parameters given by Eqs. (3) and (4), the spacecraft delay and clock epoch parameter estimate variances are given by

$$\sigma^2_{\widehat{\Delta\tau}_g,w} = \sigma^2_{sc,w} + \sigma^2_{rs,w} \tag{7}$$

$$\sigma^2_{\widehat{\Delta\tau}_c,w} = \sigma^2_{rs,w} \tag{8}$$

where $\sigma^2_{sc,w}$ and $\sigma^2_{rs,w}$ are the white components of $\langle\epsilon^2_{sc}\rangle$ and $\langle\epsilon^2_{rs}\rangle$, respectively. Note that since white observable noise is temporally uncorrelated, it is uncorrelated between the spacecraft and radio source observations.

The impact of all correlated errors affecting the delay measurements can be evaluated in a *consider* analysis (e.g., [10]). This is the formal method for determining how much a given error source cancels in the differencing of spacecraft and radio source delays prescribed by Eq. (5). The parameter estimate variances due to correlated error sources are

$$\sigma^2_{\widehat{\Delta\tau}_g,c} = \sigma^2_{sc,c} + \sigma^2_{rs,c} - 2\rho\sigma_{sc,c}\,\sigma_{rs,c} \tag{9}$$

$$\sigma^2_{\widehat{\Delta\tau}_c,c} = \sigma^2_{rs,c} \tag{10}$$

where $\sigma^2_{sc,c}$ and $\sigma^2_{rs,c}$ are due to correlated components of $\langle\epsilon^2_{sc}\rangle$ and $\langle\epsilon^2_{rs}\rangle$, respectively, and ρ is the correlation coefficient between the spacecraft and radio source observations. Familiar ΔDOR rules of thumb, such as "ΔDOR errors grow proportionally with spacecraft–radio source separation," formally originate in Eq. (9). Examples of correlated error sources are clock rate, Earth rotation, and tropospheric effects.

III. Local Reference Frame Parameter Estimation

Equations (3) through (10) cast ΔDOR in the form of a parameter estimation procedure. The parameters estimated are the residual spacecraft geometric delay and residual differential clock epoch. It has been shown that clock rate, Earth orientation, and static tropospheric effects are the next dominant correlated error sources in ϵ_{sc} and ϵ_{rs} (see reference 3). (As will be assumed throughout this article, ionospheric errors are largely removed by dual-frequency calibration and contribute less than 100-picoradian observation errors for the typical 2300- and 8400-GHz observing frequencies.) The approach taken in the reference to reduce ΔDOR uncertainties from the 30- to the 5-nanoradian level was to improve calibration

support. Highly accurate earth orientation measurements and water vapor radiometry were suggested as the means to improving ΔDOR. An alternative to augmenting calibration support is to introduce more parameters into Eqs. (3) and (4) and make more radio source observations to solve for them. As implied in the introduction, the Mark III instrumentation now being installed in the DSN will allow on the order of six highly accurate (≈30-picosecond) radio source group delay measurements to be made in the same time currently allotted for one.

In Eqs. (11) and (12) below, Eqs. (3) and (4) are rewritten with the extended parameter dependences. The first new parameter is $\dot{\tau}_c$, which is the delay due to the residual differential clock rate between the two stations. The next two parameters, θ and ϕ, are the magnitudes of rotations about two axes perpendicular to the baseline. The rotation axes are chosen to be $\hat{s}_{msc} \times \vec{B}_m$ and $\vec{B}_m \times \hat{s}_{msc} \times \vec{B}_m$. The next two parameters, z_1 and z_2, are the magnitudes of the static zenith tropospheric delay over each of the two stations. The expressions for all partial derivatives of delay with respect to those parameters are given in Appendix A. The local-reference-frame extended parameterizations for observed delay are

$$\Delta\tau_{sc} = \frac{\partial\tau_{sc}}{\partial\tau_g}\Delta\tau_g + \frac{\partial\tau_{sc}}{\partial\tau_c}\Delta\tau_c + \frac{\partial\tau_{sc}}{\partial\dot{\tau}_c}\Delta\dot{\tau}_c + \frac{\partial\tau_{sc}}{\partial\theta}\Delta\theta + \frac{\partial\tau_{sc}}{\partial\phi}\Delta\phi + \frac{\partial\tau_{sc}}{\partial z_1}\Delta z_1 + \frac{\partial\tau_{sc}}{\partial z_2}\Delta z_2 + \epsilon'_{sc} \tag{11}$$

$$\Delta\tau_{rs} = \frac{\partial\tau_{rs}}{\partial\tau_c}\Delta\tau_c + \frac{\partial\tau_{rs}}{\partial\dot{\tau}_c}\Delta\dot{\tau}_c + \frac{\partial\tau_{rs}}{\partial\theta}\Delta\theta + \frac{\partial\tau_{rs}}{\partial\phi}\Delta\phi + \frac{\partial\tau_{rs}}{\partial z_1}\Delta z_1 + \frac{\partial\tau_{rs}}{\partial z_2}\Delta z_2 + \epsilon'_{rs} \tag{12}$$

where ϵ'_{sc} and ϵ'_{rs} include all observation errors not explicitly appearing on the right sides of Eqs. (11) and (12), respectively. There are now seven parameters to be estimated.

It should be noted that the VLBI phase delay rate, which is a measure of the short-term rate of change of VLBI delay, is extracted along with the delay in the VLBI fringe fitting procedure. It is not normally used in standard ΔDOR because it is believed to be dominated by atmospheric fluctuations rather than by the geometric signature of the rotating Earth [11]. It will be seen, however, that in the local reference frame technique, the phase delay rate can be used to constrain singularities in the least squares solution for the above seven parameters. The parameter dependences of the observed residual spacecraft and radio source delay rates, $\Delta\dot{\tau}_{sc}$ and $\Delta\dot{\tau}_{rs}$, are expressed in Eqs. (13) and (14):

$$\Delta\dot{\tau}_{sc} = \frac{\partial\dot{\tau}_{sc}}{\partial\dot{\tau}_g}\Delta\dot{\tau}_g + \frac{\partial\dot{\tau}_{sc}}{\partial\tau_c}\Delta\tau_c + \frac{\partial\dot{\tau}_{sc}}{\partial\dot{\tau}_c}\Delta\dot{\tau}_c + \frac{\partial\dot{\tau}_{sc}}{\partial\theta}\Delta\theta + \frac{\partial\dot{\tau}_{sc}}{\partial\phi}\Delta\phi + \frac{\partial\dot{\tau}_{sc}}{\partial z_1}\Delta z_1 + \frac{\partial\dot{\tau}_{sc}}{\partial z_2}\Delta z_2 + \epsilon''_{sc} \tag{13}$$

$$\Delta\dot{\tau}_{rs} = \frac{\partial\dot{\tau}_{rs}}{\partial\tau_c}\Delta\tau_c + \frac{\partial\dot{\tau}_{rs}}{\partial\dot{\tau}_c}\Delta\dot{\tau}_c + \frac{\partial\dot{\tau}_{rs}}{\partial\theta}\Delta\theta + \frac{\partial\dot{\tau}_{rs}}{\partial\phi}\Delta\phi + \frac{\partial\dot{\tau}_{rs}}{\partial z_1}\Delta z_1 + \frac{\partial\dot{\tau}_{rs}}{\partial z_2}\Delta z_2 + \epsilon''_{rs} \tag{14}$$

The partial derivatives of delay rate with respect to the parameters are given in Appendix A in terms of baseline and source coordinates. The new parameter in Eq. (13) is the residual spacecraft geometric delay rate, $\Delta\dot{\tau}_g$. This parameter, inserted for completeness, represents the sum of two contributions to the spacecraft's delay rate: (1) the residual rate induced by unmodeled spacecraft motion; and (2) the residual rate induced by Earth rotation in the presence of a nonzero residual spacecraft position vector. In Eqs. (13) and (14), ϵ''_{sc} and ϵ''_{rs} are the contributions to the spacecraft and radio source delay rate not explicitly parameterized.

As will be described in the next section on covariance results, the seven parameters in Eq. (11) are largely determined by delay observations; approximately seven delay observations are therefore required in a local reference frame observing sequence with the above parameterizations. Only the $\dot{\tau}_g$ parameter is explicitly determined by the delay rate observation, and it is of minimal use in reducing angular position errors. In the next section, a data acquisition strategy is evaluated in which the spacecraft and five radio sources are observed, with one source observed twice. The error in determining residual spacecraft geometric delay due to system noise, tropospheric fluctuations, and source structure will be calculated.

IV. Covariance Results

A. Observation Configuration for Covariance Calculation

The radio source–spacecraft configuration used to calculate sample covariance results is shown in Fig. 1. The radio sources, which are denoted by *R*s in the figure, are from the DSN source catalog. Their coordinates in the J2000 reference

frame are given in Table 1 [7].[5] The S in Fig. 1 denotes the spacecraft angular position used for the covariance analyses; its coordinates are the last entry in Table 1. In these analyses, it was assumed that the spacecraft and four of the five radio sources were observed only once on the California–Australia baseline. One radio source was observed twice to provide the seven observations needed to determine the seven parameters in Eq. (11) above. The numbers below the letters in Fig. 1 indicate the temporal sequence of observations. Each observation was assumed to last one minute, with two minutes allowed for antenna slewing. In Section IVB, the covariance due to system noise and tropospheric fluctuations is presented. Section IVC contains the covariance due to source structure effects. Although the spacecraft observation was spatially and temporally centered in the sample observing sequence, the covariance results which follow do not critically depend on such a sequence. For example, observing the spacecraft before all radio source observations changes the results of the next section by only ±1 nanoradian.

B. Covariance Due to System Noise and Tropospheric Fluctuations

In order to evaluate the spacecraft angular error due to white system noise in the local reference frame example of Fig. 1, white noise standard deviations of 30 picoseconds were assumed for both the radio source and spacecraft observations. For the selected radio sources, this assumption is consistent with typical Mark III group delay noise values for one-minute observations. If it were possible to use the higher-precision VLBI phase delays instead of group delays [12], then typical noise standard deviations would be below one picosecond. However, this analysis will not assume the availability of the phase delay data type. Using standard least squares techniques, an equation analogous to Eq. (7) can be derived for the spacecraft geometric delay error in terms of the system noise contributions of the seven observations described above.

The model described in Eqs. (11) through (14) assumes a static tropospheric delay over each station. Tropospheric fluctuations, predominantly due to the wet component, will cause an error in the spacecraft geometric delay. This error has been evaluated in a consider analysis using a covariance matrix, derived for average DSN conditions, from wet tropospheric fluctuation modeling ([11], Eq. [15]). The model in the reference assumes that a frozen spatial pattern of turbulence is blown across a site by the wind. The model, which is normalized by WVR data taken near Goldstone, is consistent with a daily wet zenith delay fluctuation of 1 cm.

[5] The first source in the table was observed too recently to appear in the publication referenced, but its coordinates are derived from the same analysis as the other sources in the table.

Both system noise and tropospheric contributions to spacecraft angular error are shown in Fig. 2. The ordinate is the error in the estimation of Δs_p of Eq. (1) for the California–Australia baseline, which is approximately 10,600 km. This angular error is plotted versus hour angle, which is defined as the angle between the spacecraft and baseline vectors at the middle of the seven-observation sequence. The pattern of Fig. 1, therefore, moves across the sky to the west as the hour angle decreases. It can be seen that the system noise contribution is between 1 and 3 nanoradians. The tropospheric error is somewhat smaller. The peak on the right side of the plot is due largely to correlations between the first rotation parameter and the clock epoch. The location and strength of such peaks are completely dependent on the baseline vector and observation schedule used. In the example of Fig. 2, if delay rates had not been used to constrain the solution, the peak would have risen to about 20 nanoradians. The solution could also have been controlled by readily achieved a priori constraints on the Earth rotation and tropospheric parameters on the order of 500 nanoradians and 4 cm, respectively. In the covariances in this article, the delay rate constraints were chosen to avoid placing specific demands on a priori knowledge; but in an operational mode, some combination of delay rates and a priori constraints could be used to control singularities in the determination of geometric delay.

In order to compare the local reference frame technique to a standard ΔDOR observing sequence, in which Earth rotation and static tropospheric effects are not estimated, these effects have been evaluated for a spacecraft and single radio source observation sequence. The radio source used was the one closest to the spacecraft (about 10 degrees away) in Fig. 1, P0019+058. Earth rotation uncertainties of 50 nanoradians per component and tropospheric zenith delay uncertainties of 4 cm were used for the consider analysis. The above Earth rotation uncertainty is typical of what will be delivered to the DSN for the Galileo and Magellan missions. The tropospheric uncertainty of 4 cm reflects the error in wet zenith delay calibration derived from surface meteorology. Figure 3 shows the contributions of these two error sources as a function of hour angle. Comparison with the local reference frame system noise error of Fig. 2, shown in Fig. 3 as a broken line, shows that estimating Earth orientation and tropospheric parameters in the multisource observation strategy reduces the tracking error due to these effects by an approximate factor of 3 for most hour angles.

C. Covariance Due to Radio Source Structure

In this subsection, the effect of time-invariant radio source structure will be discussed. Time-varying source structure will be mentioned in Section V, but no detailed method for minimizing its effect is given in this article. If the absolute location of the spacecraft is required in the radio frame, radio source

structure at the 5-nanoradian level imposes a serious limitation. In the observation configuration of Section A, the absolute measurement of spacecraft location is degraded to the 10-nanoradian level due to 5-nanoradian, time-invariant source position errors caused by structure effects. Radio source maps could be made at regular intervals to calibrate the structure effects, but that effort would be costly and in contrast to the self-contained nature of the local reference frame technique. However, as will be shown below, uncalibrated source structure effects can be dramatically reduced for relative angular measurements. In many applications, measurement of the spacecraft's change in angular position over some period of time can provide valuable navigation information. The stability of typical radio source structures over 6-month to 1-year periods can then be exploited. Because the induced signature of constant source structure over these time periods is largely the same, it cancels in the relative position measurement. This statement is treated rigorously in Appendix B on stationary source structure, in which it is shown that maximum error canceling between observations is facilitated by using the same observation sequence.

Using the same observation sequence helps in two ways: (1) time-invariant source structure effects on each delay and delay rate observation will repeat because the projection of the source component vectors onto the baseline will repeat; and (2) as shown in Appendix B, observable errors which are completely correlated will largely cancel in the differencing of sequential spacecraft position measurements if the partial derivatives and system noise covariances are similar. The time-invariant structure effect will be identically zero if exactly the same observation sequence is used. Using similar observation sequences means that the spacecraft position cannot change substantially or the parameter estimation formalism, which leads to the multisource analog of Eq. (5), will propagate the structure effect differently from one angular determination to the next. This means that, in order to minimize the source structure effect and achieve the few-nanoradian relative angular accuracy suggested by Fig. 2, the spacecraft cannot move significantly in the sky between measurements, which is a typical geometry for an outer planet encounter.

In Fig. 4, the source structure effect on relative angular measurements is shown, assuming that the spacecraft moved from the S to the indicated points on the two circles between measurements. An apparent error of 5 nanoradians in radio source position due to structure was assigned for $\alpha \cos \delta$ and δ, where α is right ascension and δ is declination, for all radio sources. This error is random from source to source, but does not vary from epoch to epoch. For the smaller, 3-degree circle, which represents approximately 40 days of travel time for asymptotic speeds of 10 km/sec, 1- to 3-nanoradian errors in spacecraft position estimates are incurred due to source structure. For the larger, 6-degree circle, source structure errors grow to between 2 and 7 nanoradians. This error growth as the spacecraft moves from its initial position is a result of the changing least squares equations, as mentioned above.

V. Summary, Improvements, and Demonstrations

In the absence of radio source structure, the covariance analyses presented here show that VLBI observations of approximately five radio sources along with a spacecraft can yield 2- to 3-nanoradian tracking results. This accuracy, based on Mark III radio source measurement noise levels, is attainable through use of the radio source observations to solve for clock, Earth orientation, and static tropospheric effects. In addition to system noise, the error contributions from tropospheric fluctuations and radio source structure uncertainties have been evaluated in consider analyses. While the tropospheric fluctuation error contributions are smaller than errors due to the assumed VLBI system noise, radio source structure can contribute up to 10 nanoradians to the error in locating a spacecraft relative to the radio frame. However, this error source can be reduced to approximately 2 nanoradians in many applications where the relative spacecraft angle over small pieces of the sky is of interest. It has been shown elsewhere (see footnote 1) that using a 2-nanoradian differential measurement to sense Jupiter's gravitational field yields target relative tracking accuracies competitive with onboard optical navigation. However, subnanoradian accuracies will be necessary to use the same technique at Neptune, for example, and improvements to the technique should be considered.

Improvements to the technique could result from reducing the error contributions from system noise, tropospheric fluctuations, and source structure. As has been mentioned above, using the highly accurate phase delay will reduce system noise contributions almost two orders of magnitude. This would mean that system noise would contribute on the order of 20 picoradians to the local reference frame technique. Obtaining phase delay data is challenging in that it requires resolving cycle ambiguities at 8400 GHz or higher radio frequencies. Resolving cycle ambiguities is theoretically possible with the Mark III system and DSN instrumentation,[6] but this capability has not yet been demonstrated on intercontinental baselines. Even if it is demonstrated, the accuracy inherent in the phase delay would be of marginal use if the other error sources considered above remained at the quoted levels.

[6] C. D. Edwards, K. M. Liewer, C. S. Jacobs, and R. N. Treuhaft, "An Algorithm for Connection of RF Phase in VLBI," JPL Interoffice Memorandum No. 335.3-475 (internal document), Jet Propulsion Laboratory, Pasadena, California, November 20, 1986.

The obvious means of reducing the tropospheric fluctuation error is by using water vapor radiometers (WVRs) [13]. Since typical water vapor fluctuations on 30-minute time scales are on the order of 5 mm [11], the WVR will have to track fluctuations at or below the millimeter level to substantially reduce the fluctuation contribution to the tracking error. WVR comparisons with spectral hygrometers, which have been conducted in the Advanced Systems Program, suggest the possibility of that precision. Note that apparent zenith delay biases in the WVR measurement, which have been suggested by some existing WVR data [14], might be tolerated as long as they could be parameterized and estimated in place of the zenith parameters appearing in Eqs. (11) through (14).

If WVRs were successfully applied to remove wet tropospheric fluctuation errors, the dry fluctuations, which are estimated to be about 25 percent of the wet on the time scale of the observation sequence, would then limit the angular measurement to approximately 300 picoradians. A possible albeit unexplored method of reducing the dry fluctuation effect is to measure unmodeled phase fluctuations on Earth-orbiting satellites to sense the dry component. Barometric arrays should also be considered. Another possibility for improving the angular measurement accuracy beyond 300 picoradians is to put an interferometric system on an orbiting platform or on the moon. In that case, the Earth rotation parameters in the system discussed here would be replaced by parameters describing the orientation of the platform or the moon. Since the variations of these parameters may be very different from Earth orientation parameters, the entire local reference frame strategy could conceivably be altered, perhaps ultimately reverting back to a single-radio-source ΔDOR strategy if platform orientation can be modeled at the 20-picoradian level.

It has been shown that tracking errors due to time-invariant radio source structure can be greatly reduced in relative measurements over small pieces of the sky. If tracking relative angular position is needed over long periods of time, the assumption that the source structure is stationary may not be valid. In these cases, it may be possible to parameterize source structure evolution[7] and use the accumulated VLBI data to estimate and remove the structure effect. The feasibility of this technique will be explored as soon as a data base on structure effects can be accumulated.

If, some time in the future, the target ephemeris is known to the few-nanoradian level in the radio reference frame, it may be desirable to have absolute rather than the differential angular measurements discussed above. In other words, determinations of a spacecraft's position relative to the radio sources may be preferable to determinations of its position relative to previous positions. As already mentioned, 10-nanoradian absolute errors can be expected from source structure in the local reference frame technique. Parameterization of source structure may again be a possibility. Another approach for decreasing structure-related errors is to use the capability of the Mark III system to detect a much larger set of weaker radio sources and select only the most pointlike of those sources. The trade-off between source structure effects and system noise errors will have to be evaluated in this approach. It may also be possible to use the structure information obtained by observing programs on the Very Long Baseline Array [15] to calibrate the structure of sources used in local reference frames.

A potentially important error source which has not been considered in this analysis is that of dispersive phase effects across the bandpasses of the receiving instrumentation. Because the spacecraft signal is a tone and the radio sources are broadband noise, variations in the phase response across the bandpass will introduce tracking errors. There may be ways to include static bandpass error into the parameter estimation scheme. It is also possible that digital front-end electronics being explored in the Advanced Systems Program for the DSN will allow calibration or elimination of this effect.

Demonstrations of the local reference frame technique are under way to test the assumptions of the covariance analysis in this report. Three experiments using the Mark III system have been conducted between California and Australia. In the first experiment, conducted on March 21, 1988, the gravitational bend by Jupiter of the ray path of the radio source P0201+113 was investigated using the local reference frame technique. This gravitational shift in angular position of about 10 nanoradians simulates a spacecraft motion of about 8 km at Jupiter. On April 2 and May 16, when Jupiter was far from the ray path, P0201+113 was observed again in the same local reference frame of radio sources. About five other groups of radio sources were also observed to test the technique. At the time of this report, fringes have been found for the first two experiments with the Block II correlator at Caltech. However, the accuracy of the measurements and the resulting significance of the detection of gravitational bending are as yet undetermined.

If the technique described is validated in a non-real-time mode through experiment, an important practical operational issue will be the transport of large data volumes in real time. As opposed to the current VLBI operational system, which relays 500 kbits/sec from the stations, the Mark III system

[7] J. S. Ulvestad, "Possible Source Structure Effects in IRIS Data," JPL Interoffice Memorandum No. 335.3-88-15 (internal document), Jet Propulsion Laboratory, Pasadena, California, February 3, 1988.

needed to achieve the derived accuracies will require transportation of approximately 50 to 100 Mbits/sec. Although the Advanced Systems demonstrations of the local reference frame technique will not be done in real time, a real-time operational system would have to employ relay satellites or optical fiber links. Data transport rather than analysis will probably be the most time-consuming step in producing tracking results for navigation.

Acknowledgments

I would like to thank the following people who made valuable contributions to the formulation presented in this article: C. D. Edwards for independent checks on some of the numerical results and comments on the manuscript; T. M. Eubanks for interpretations of local reference frame geometry; J. S. Border and J. S. Ulvestad for critical readings of the manuscript; G. E. Lanyi for clarifying relevant aspects of linear algebra; C. L. Thornton for suggesting techniques for understanding poorly determined parameter estimates; and J. L. Fanselow for initially encouraging investigation into a multisource observation strategy.

References

[1] J. S. Border, F. F. Donivan, S. G. Finley, C. E. Hildebrand, B. Moultrie, and L. J. Skjerve, "Determining Spacecraft Angular Position With Delta VLBI: The Voyager Demonstration," *AIAA Paper 82-1471*, 1982.

[2] A. E. E. Rogers et al., "Very-Long-Baseline Radio Interferometry: The Mark III System for Geodesy, Astrometry, and Aperture Synthesis," *Science*, vol. 219, pp. 51-54, 1983.

[3] J. K. Miller and K. H. Rourke, "The Application of Differential VLBI to Planetary Approach Orbit Determination," *DSN Progress Report 42-40*, pp. 84-90, May 1977.

[4] T. Gold, "Radio Method for the Precise Measurement of the Rotation Period of the Earth," *Science*, vol. 157, pp. 302-304, July 1967.

[5] A. E. E. Rogers, "Very Long Baseline Interferometry With Large Effective Bandwidth for Phase-Delay Measurements," *Radio Science*, vol. 5, pp. 1239-1247, October 1970.

[6] J. B. Thomas, "An Analysis of Long Baseline Radio Interferometry," *JPL Technical Report 32-1526*, vol. VII, Jet Propulsion Laboratory, Pasadena, California, pp. 37-50, 1972.

[7] O. J. Sovers, C. D. Edwards, C. S. Jacobs, G. E. Lanyi, K. M. Liewer, and R. N. Treuhaft, "Astrometric Results of 1978–85 Deep Space Network Radio Interferometry: The JPL 1987-1 Extragalactic Source Catalog," *Astronomical Journal*, vol. 95, pp. 1647-1658, June 1988.

[8] J. S. Ulvestad, "Effects of Source Structure on Astrometry and Geodesy," in *Proc. of IAU Symposium No. 129*, pp. 429-430, 1987.

[9] W. C. Hamilton, *Statistics in Physical Science*, New York: Ronald Press, pp. 124–132, 1964.

[10] G. J. Bierman, *Factorization Methods for Discrete Sequential Estimation*, New York: Academic Press, p. 169, 1977.

[11] R. N. Treuhaft and G. E. Lanyi, "The Effect of the Dynamic Wet Troposphere on Radio Interferometric Measurements," *Radio Science*, vol. 22, pp. 251–265, March 1987.

[12] C. D. Edwards, "Short Baseline Phase Delay Interferometry," *TDA Progress Report 42-91*, vol. July–September 1987, Jet Propulsion Laboratory, Pasadena, California, pp. 46–56, November 15, 1987.

[13] G. M. Resch, D. E. Hogg, and P. J. Napier, "Radiometric Correction of Atmospheric Path Length Fluctuation in Interferometric Experiments," *Radio Science*, vol. 19, pp. 411–422, 1984.

[14] D. M. Tralli, E. C. Katsigiris, and T. H. Dixon, "Estimation of Wet Tropospheric Path Delays in GPS Baseline Solutions for the 1986 Caribbean Experiment," *EOS*, vol. 69, p. 332, April 1988.

[15] J. D. Romney, "The Very Long Baseline Array," in *Proc. of IAU Symposium No. 129*, 1987.

[16] G. E. Lanyi, "Tropospheric Calibration in Radio Interferometry," in *Proc. Int. Symp. Space Tech. Geodyn., IAG/COSPAR*, vol. 2, pp. 184–195, 1984.

[17] J. L. Davis, T. A. Herring, I. I. Shapiro, A. E. E. Rogers, and G. Elgered, "Geodesy by Radio Interferometry: Effects of Atmospheric Modeling Errors on Estimates of Baseline Length," *Radio Science*, vol. 20, pp. 1593–1607, 1985.

Table 1. Radio source and spacecraft positions used for local reference frame covariance analysis

Radio source name	Right ascension, hours/minutes/seconds			Declination, degrees/minutes/seconds		
P0048−09	0	50	41.3180	−9	29	5.216
P0019+058	0	22	32.4413	6	8	4.272
P0106+01	1	8	38.7711	1	35	0.320
P2320−035	23	23	31.9538	−3	17	5.022
P2345−16	23	48	2.6085	−16	31	12.019
Spacecraft	0	20	0.0000	−5	0	0.000

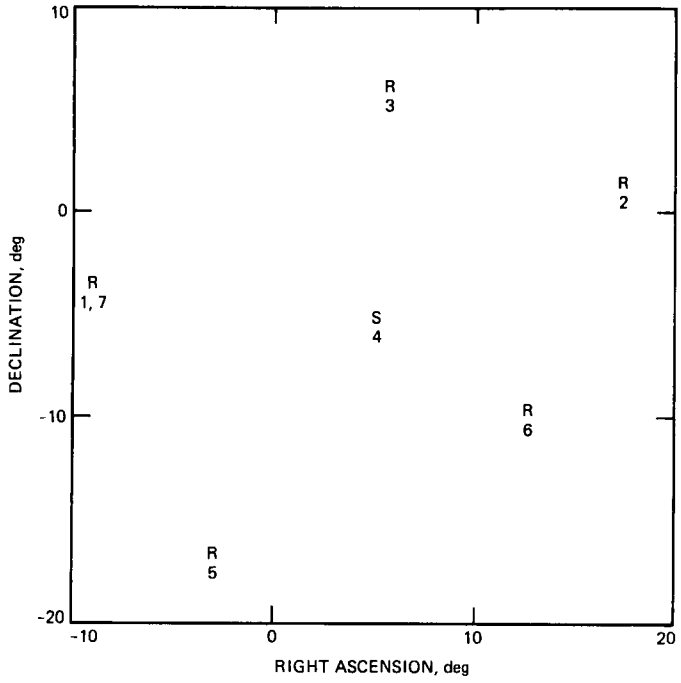

Fig. 1. The radio source and spacecraft angular distribution used in all covariance analysis results of Section III. In that section, only the California–Australia baseline is considered.

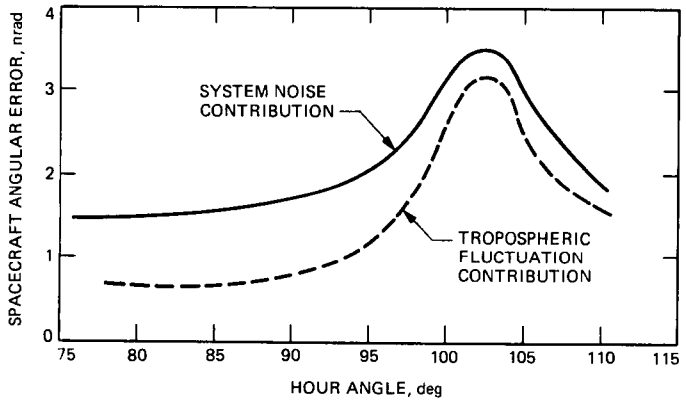

Fig. 2. Local reference frame covariance results: the spacecraft angular error (Δs_p of Eq. [1]) due to system noise of 30 picoseconds per observation and 1-cm daily zenith wet tropospheric fluctuations, as a function of hour angle. The hour angle is the angle between the spacecraft and the baseline at the middle of the 7-observation sequence.

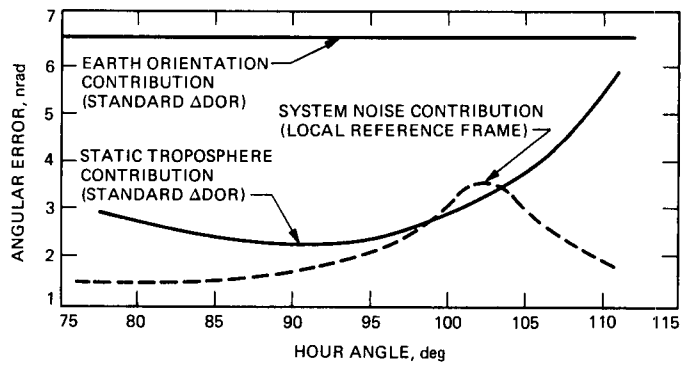

Fig. 3. Standard ΔDOR covariance results: the standard ΔDOR (single radio source) angular error due to 50-nanoradian Earth orientation uncertainty and 4-cm tropospheric delay uncertainty. For comparison, the dashed line is the local reference frame system noise covariance from Fig. 2.

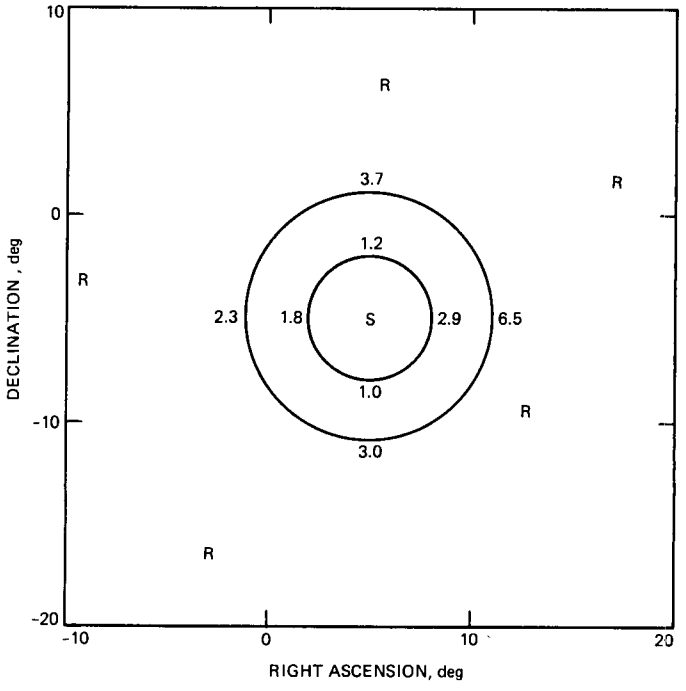

Fig. 4. Differential angular position error due to stationary source structure: the numbers indicate the error, in nanoradians, in a measurement of relative spacecraft position due to time-invariant source structure errors. The numbers apply to a differential position measurement between the *S* and the indicated point on the circle. All radio sources were assumed to have 5-nanoradian errors in $\alpha \cos \delta$ and in δ where α is right ascension and δ is declination.

Appendix A
Partial Derivatives of Delay and Rate

In the case of standard ΔDOR, the partial derivatives of observed delay with respect to the spacecraft and clock delay parameters, $\partial\tau_{sc}/\partial\tau_g$ and $\partial\tau_{sc}/\partial\tau_c$, are unity. Below, the partial derivatives with respect to all the additional parameters in Eq. (11) are expressed in terms of source and baseline components and observation epochs. The partial derivatives of delay rate are similarly treated. Since the only differences between a spacecraft and radio source observation in this treatment are the objects' angular positions and the observation epochs, the partial derivatives below apply to either type of observation. The subscripts *sc* and *rs* in Eqs. (11) and (12) will therefore be ignored. Five partial derivatives, one for each parameter added in the local reference frame approach, are given below. The derivatives are of delay with respect to station-differenced clock rate, two rotation angles, and two zenith tropospheric delays.

The partial derivative of observed delay with respect to station-differenced clock rate is

$$c\frac{\partial\tau}{\partial\dot{\tau}_c} = t - t_0 \tag{A-1}$$

where t is the observation epoch and t_0 is the average of all spacecraft and radio source observation epochs.

The first Earth rotation partial derivative in Eq. (11) is as follows:

$$\begin{aligned}\frac{\partial\tau}{\partial\theta} = {} & B_{m\,x|t}(\cos\delta\ \sin\alpha\ \sin\delta_c - \sin\delta\ \cos\delta_c\ \sin\alpha_c) \\ & + B_{m\,y|t}(\sin\delta\ \cos\delta_c\ \cos\alpha_c - \cos\delta\ \cos\alpha\ \sin\delta_c) \\ & + B_{m\,z|t}(\cos\delta\ \cos\delta_c\ \sin(\alpha_c - \alpha))\end{aligned} \tag{A-2}$$

where, as defined in the text, θ is the magnitude of a rotation about the $\hat{s}_{m\,sc} \times \vec{B}_m$ axis, where $\vec{B}_m$ is the a priori baseline vector at the spacecraft observation epoch. Note that $B_{m\,x|t}$, $B_{m\,y|t}$, and $B_{m\,z|t}$ are the a priori baseline components, in a space-fixed coordinate system, evaluated at the time t at which τ is measured. In Eq. (A-2), α, δ, α_c, and δ_c are the right ascensions and declinations of the observed source and the rotation axis, respectively. The partial derivative of delay with respect to ϕ, the magnitude of the rotation about $\vec{B}_m \times \hat{s}_{m\,sc} \times \vec{B}_m$, is given by an expression identical to Eq. (A-2) with α_c and δ_c replaced by the right ascension and declination of the $(\vec{B}_m \times \hat{s}_{m\,sc} \times \vec{B}_m)$ vector.

The partial derivative of observed delay with respect to observed station 1's zenith troposphere delay is given by

$$\frac{\partial\tau}{\partial z_1} = \frac{-1}{\sin\gamma_1} \tag{A-3}$$

where γ_1 is the elevation angle at station 1. The error in covariance results incurred by not using a more realistic zenith partial derivative is about 0.1 nanoradian. When subnanoradian accuracies are attempted, the dry and wet troposphere, each with its own mapping functions [16], [17], will need more careful treatment than implied by Eq. (A-3). An expression for the partial derivative of geometric delay with respect to station 2's zenith troposphere is obtained by substituting 2 for 1 in Eq. (A-3) and omitting the minus sign.

The partial derivatives of delay rate with respect to the model parameters of Eqs. (13) and (14) are given below. The first three derivatives of rate with respect to spacecraft geometric rate and clock parameters are

$$\begin{aligned}\frac{\partial\dot{\tau}}{\partial\dot{\tau}_g} &= 1 \\ \frac{\partial\dot{\tau}}{\partial\tau_c} &= 0 \\ \frac{\partial\dot{\tau}}{\partial\dot{\tau}_c} &= 1\end{aligned} \tag{A-4}$$

where all symbols are defined in the text. The first line of Eq. (A-4) applies to the spacecraft rate observation only, as the partial of radio source observed rate with respect to spacecraft geometric rate is zero. Eq. (A-4) states that delay rate parameters map directly into delay rate observations, and the value of the clock epoch parameter does not affect the delay rate observations.

Because an important component of the modeled geometric delay rate is due to baseline rotation about the Earth's spin axis, baseline orientation errors cause residual observed delay rate. The partial derivatives are found by performing an infinitesimal rotation on the baseline and calculating the difference in delay rate between the rotated and original baseline. For a rotation about the $\hat{s}_{m\,sc} \times \vec{B}_m$ axis, with rotation axis right

ascension and declination α_c and δ_c, the delay rate partial derivative is

$$c\frac{\partial\dot{\tau}}{\partial\theta} = \Omega\cos\delta$$
$$\times\left[\cos\alpha\,(B_{m\,z|t}\cos\delta_c\ \cos\alpha_c - B_{m\,x|t}\sin\delta_c)\right.$$
$$\left.+\sin\alpha\,(B_{m\,z|t}\cos\delta_c\ \sin\alpha_c - B_{m\,y}\sin\delta_c)\right] \qquad \text{(A-5)}$$

where Ω is the Earth's rotation rate in radians/sec. A similar expression holds for $\partial\tau/\partial\phi$.

For the partial derivatives of delay rate with respect to zenith delay, the troposphere is taken to be static. That is, the rate signature is again induced by Earth rotation, which causes an elevation angle rate. The partial derivative is found numerically by calculating elevation angles at plus and minus two seconds from the observation epoch. The rate of change of Eq. (A-3) is thereby obtained.

Appendix B

The Effect of Stationary Radio Source Structure on Differential Angular Position Determinations

As noted in Section IVC, time-invariant source structure has less effect on differences in angular position than on absolute angular position in the radio frame. In this appendix, the the effect of time-invariant source structure on the angular difference determination is evaluated. Figure 4 results from the derivation below. The treatment applies equally well to radio source position errors, because the source structure errors can be represented by unknown shifts in the effective radio source positions. For the source structure calculation, it will be assumed that the observing schedule for the radio sources is identical for the two local reference frame measurements. The spacecraft will be allowed to move. Its observation epoch will be taken to be identical for the two measurements, but its position on the sky (and therefore relative to the baseline) will be allowed to change. For the following calculation, the effect of constant but unknown errors on a general parameter estimate, $\hat{X}_i$, will be considered. This generalized notation is consistent with the index manipulations in the derivation. For the relative tracking problem in question, $\hat{X}_i$ should be thought of as the residual spacecraft geometric delay parameter.

In the linear least squares formalism, the estimate of the ith parameter, $\hat{X}_i$, is given by

$$\hat{X}_i = \sum_{j=1,N} F_{i,j}\, \Delta\tau_j \tag{B-1}$$

where N is the number of observations and the $\Delta\tau_j$s are the residual observation delays due solely to source structure effects. The $F_{i,j}$s are the least squares coefficients which describe the contribution of the jth observation to the ith parameter estimate; they are explicitly defined in Eq. (B-3) below. Equation (5) in the text is an example of Eq. (B-1) for the specific case of ΔDOR. An estimate of the same parameter, from observations at a later epoch, will be denoted by

$$\hat{X}'_i = \sum_{j=1,N} F'_{i,j}\, \Delta\tau_j \tag{B-2}$$

The $\Delta\tau_j$ terms are not primed because it is assumed that they arise from the same source structure or uncertainty effects for both the unprimed and primed observations. Although the parameter estimates in this appendix are derived from $\Delta\tau_j$ delay measurements only, this treatment can be extended by including delay rates in Eqs. (B-1) and (B-2). The $F_{i,j}$ and $F'_{i,j}$ coefficients are given by [9]

$$\begin{aligned} F_{i,j} &= \left[(A^T W A)^{-1} A^T W\right]_{i,j} \\ F'_{i,j} &= \left[(A'^T W A')^{-1} A'^T W\right]_{i,j} \end{aligned} \tag{B-3}$$

The matrix A is defined by $A_{m,n} = \partial\tau_m/\partial X_n$. The A matrix includes the partial derivatives calculated in the previous appendix. If the spacecraft has moved between the unprimed and primed observations, then the partial derivatives of spacecraft delay with respect to model parameters in the A' matrix will be different from those in the A matrix; all other elements of A and A' will be identical to each other. In Eq. (B-3), W is the inverse of the modeled observable covariance matrix. It has been assumed that the modeled observable covariances, such as system noise, do not change between the unprimed and primed observations. Although this need not be assumed to complete the derivation, the modeled covariances would generally be nearly identical for each observation set.

In order to calculate the variance of relative $\hat{X}_i$ determinations due to source structure, the $\Delta\tau_j$'s will be associated with geometric delay errors induced by position uncertainties. Below, $\Delta\tau_j$ is written in terms of parameter residuals ΔP_k:

$$\Delta\tau_j = \sum_k \frac{\partial\tau_j}{\partial P_k}\, \Delta P_k \tag{B-4}$$

where the P_k parameters are the right ascensions and declinations of the observed radio sources. Obviously, the partial derivative in Eq. (B-4) vanishes unless P_k is the right ascension or declination of the radio source being observed in the jth VLBI delay measurement.

The variance of $(\hat{X}_i - \hat{X}'_i)$ in terms of the covariance of the P_k source coordinate parameters will now be calculated. Expressions for the variance of $\hat{X}_i$ will be needed. From Eqs. (B-1) and (B-4), it is

$$\text{var}\,(\hat{X}_i) = \sum_{j,k,l,m} F_{i,j}\, \frac{\partial\tau_j}{\partial P_k}\, M_{p\,k,l}\, \frac{\partial\tau_m}{\partial P_1}\, F_{i,m} \tag{B-5}$$

where $M_{p\,k,l}$ is the covariance of the kth and lth source coordinate errors. Expressions similar to Eq. (B-5) can be derived for the variance of $\hat{X}_i'$ and the covariance of $\hat{X}_i$ and $\hat{X}_i'$, leading to the final result, shown below in matrix form:

$$\text{var}\,(\hat{X}_i - \hat{X}_i') = (FDM_pD^TF^T)_{i,i} + (F'DM_pD^TF'^T)_{i,i} - 2\,(FDM_pD^TF'^T)_{i,i} \qquad \text{(B-6)}$$

where $D_{i,j} \equiv \partial\tau_i/\partial P_j$.

Equation (B-6) illustrates the parameter error cancellation which can arise when parameter estimates are differenced in the presence of unknown but repeatable errors. If the observing schedules were exactly the same—that is, if the spacecraft did not move at all on the sky—then all primed quantities would equal all unprimed quantities and Eq. (B-6) would yield identically zero. Small changes in spacecraft position make small differences between the F and F' and A and A' matrices, yielding the results of Fig. 4.[8] Note that the crucial step in realizing the cancellation was assuming that the $\Delta\tau_j$'s were identical for the unprimed and primed measurements. This is equivalent to saying that the source structure or position uncertainties did not change from one observation to the next.

[8] The actual calculation of the results for Fig. 4 employed the generalization of Eq. (B-6), which includes both delay and delay rate observations.